

1 **Title:** Single cell analysis identifies *CRLF2* rearrangements as both early and late events  
2 in Down syndrome and non-Down syndrome acute lymphoblastic leukaemia

3

4 **Authors:** \*Potter N<sup>1</sup>, \*Jones L<sup>2</sup>, Blair H<sup>2</sup>, Strehl S<sup>3</sup>, Harrison CJ<sup>2</sup>, Greaves M<sup>1</sup>, Kearney  
5 L<sup>1</sup>, Russell LJ<sup>2</sup>

6 <sup>1</sup>The Institute of Cancer Research, London, UK;

7 <sup>2</sup>Northern Institute for Cancer Research, Newcastle University, Newcastle-upon-Tyne,  
8 UK;

9 <sup>3</sup>CCRI, Children's Cancer Research Institute, St. Anna Kinderkrebsforschung, Vienna,  
10 Austria.

11 \* These authors contributed equally to this work

12 **Corresponding author:** Dr. Lisa J Russell, Northern Institute for Cancer Research, Level  
13 6, Herschel Building, Brewery Lane, Newcastle upon Tyne, NE1 7RU, UK.

14 Tel: +44 (0)191 2082235

15 Email: lisa.russell@newcastle.ac.uk

16 **Running Title** - *CRLF2* rearrangements are both early and late events

17 **Conflict of Interest** - All authors have no conflicts of interest to disclose.

18 **Sources of support** – Financial support from Kay Kendall Leukaemia Fund, Children  
19 with Cancer UK, Bloodwise, Wellcome Trust, Leuka and the North of England's  
20 Children's Cancer Research Fund.

21

22

23

24

25

26

27 **Abstract**

28 Deregulated expression of the type I cytokine receptor, *CRLF2*, is observed in 5-15%  
29 of precursor B-cell acute lymphoblastic leukaemia (B-ALL). We have previously  
30 reported the genomic landscape of patients with *CRLF2* rearrangements (*CRLF2*-r)  
31 using both whole genome and exome sequencing, which identified a number of  
32 potential clonal and sub-clonal genomic alterations. In this study, we aimed to assess  
33 when the *CRLF2*-r; *IGH-CRLF2* or *P2RY8-CRLF2*, arose during the evolution of both  
34 Down syndrome-ALL (DS-ALL) and non-DS-ALL. Using fluorescence *in situ*  
35 hybridisation, we were able to track up to four structural variants in single cells from  
36 47 *CRLF2*-r B-ALL patients, which in association with our multiplex single cell analysis  
37 of a further four patients, permitted simultaneous tracking of copy number  
38 alterations, structural and single nucleotide variants within individual cells. We  
39 observed *CRLF2*-r arising as both early and late events in DS and non-DS-ALL patients.  
40 Parallel evolution of discrete clones was observed in the development of *CRLF2*-r B-  
41 ALL, either involving the *CRLF2*-r or one of the other tracked abnormalities. In depth  
42 single cell analysis identified both linear and branching evolution with early clones  
43 harbouring a multitude of abnormalities, including the *CRLF2*-r in DS-ALL patients.

44

45

46

47

48

49 **Introduction**

50 Acute lymphoblastic leukaemia (ALL) is defined by primary chromosomal  
51 abnormalities that drive disease development and progression and are strongly  
52 associated with outcome (1). However, the impact of sub-clonal architecture,  
53 including structural variants and mutations, is not as well defined. Initial insights into  
54 secondary genetic changes were gained through the study of monozygotic twins in  
55 which either one or both children developed ALL (2-5). These investigations identified  
56 an *in utero* origin of ALL. In particular, pre-leukaemic clones were found to harbour  
57 the *ETV6-RUNX1* fusion, which required additional abnormalities after birth to lead to  
58 overt leukaemia. Key features of the sub-clonal architecture of these cases suggested  
59 a Darwinian natural selection model to describe the process through which leukaemia  
60 presents, progresses and evades treatment (2, 3, 6).

61 Initiating genomic abnormalities have not been described in all subgroups of B-lineage  
62 ALL (B-ALL). A particular subtype, known as Ph-like/*BCR-ABL1*-like ALL, constitutes 10-  
63 15% of B-ALL (7, 8). It is characterised by; a transcriptional profile similar to *BCR-ABL1*  
64 driven disease; high expression of the type I cytokine receptor, *cytokine receptor-like*  
65 *factor 2 (CRLF2)*; the presence of tyrosine kinase activating fusion genes and mutations  
66 of genes within the JAK/STAT and RAS signalling pathways (9). Deregulation of *CRLF2*  
67 occurs via two genomic alterations (*IGH-CRLF2*, *P2RY8-CRLF2*) resulting in its  
68 overexpression, however on their own they are insufficient to cause overt leukaemia  
69 (10-12). It is well documented that copy number alterations of genes involved in B-cell  
70 differentiation and cell cycle control (10, 13-15), including *PAX5*, *IKZF1* and *CDKN2A*,  
71 and mutations of kinases or receptor encoding genes (9, 16), in particular *CRLF2*, *JAK2*

72 and *IL7R*, are common in this subtype of B-ALL. However, data indicating whether  
73 *CRLF2*-rearrangements (*CRLF2-r*) are early and/or sub-clonal event are scarce (17, 18).  
74 Evidence of intratumoral heterogeneity has been revealed by a range of techniques,  
75 including conventional cytogenetics (19) and fluorescence in situ hybridisation (FISH)  
76 (20). Next generation sequencing technologies have exposed remarkable complexities  
77 in the genomic landscape of leukaemic blasts (21); coupling this approach with single  
78 cell analysis revealed additional multiple levels of heterogeneity that may further  
79 inform of treatment failure, resistance and subsequent relapse (22, 23).

80 In this respect, we have previously developed a multiplex Q-PCR method to target  
81 patient specific DNA alterations in flow-sorted single leukaemic cells using the  
82 BioMark HD microfluidics platform (23). This approach allows the simultaneous  
83 detection of structural variants (SVs), including translocations and fusion genes, copy  
84 number alterations (CNAs) and single nucleotide variants (SNVs) within a single cell  
85 that can be combined to illustrate clonal evolution within a bulk sample (20, 24, 25).

86 We have previously reported the genomic landscape of 11 *CRLF2-r* patients, using  
87 both whole genome (WGS) and exome sequencing (WES) (26), which identified a  
88 number of potential driver genomic alterations in each case. Both read counts and  
89 variant allele frequencies varied, suggesting that some aberrations were sub-clonally  
90 distributed, whilst others were clonal. In this study, we aimed to assess at what time  
91 point the *CRLF2-r*; *IGH-CRLF2* or *P2RY8-CRLF2*, arose in the evolution of both Down  
92 syndrome-ALL (DS-ALL) and non-DS-ALL. Using FISH, we were able to track up to four  
93 SVs in single cells from 47 *CRLF2-r* ALL patients, which in association with multiplex  
94 single cell analysis of a further four patients, has permitted simultaneous tracking of  
95 CNAs, SVs and SNVs within single cells.

96 In this study, we have observed *CRLF2*-r arising as both early and late events in DS and  
97 non-DS-ALL. Parallel evolution of discrete clones was observed in the development of  
98 *CRLF2*-r ALL, either involving the *CRLF2*-r or one of the other tracked abnormalities. In  
99 depth single cell analysis identified both linear and branching evolution with early  
100 clones harbouring a multitude of abnormalities, including the *CRLF2*-r in DS-ALL.

101

## 102 **Methods**

### 103 **Sample Cohort**

104 Patients with a *CRLF2*-r detectable by FISH or Multiplex Ligation-dependent Probe  
105 Amplification (MLPA) with available material were selected from six ALL treatment  
106 trials: UKALL97/99, n=24; UKALL2003, n=16; UKALLXI, n=2; UKALLXII, n=6; UKALLR3,  
107 n=1; ALL-BFM 2000, n=2 (Supplementary Table 1). Ages ranged from 1-54 years  
108 (median 5 years, mean 9.73 years).

109 Institutional review board approval was obtained at each of the collaborating centres.

110 Informed consent was obtained in accordance with the Declaration of Helsinki.

### 111 **Genomic target selection**

112 WGS and WES data for the patients included in this study have been previously  
113 published (26). We used these data to identify SVs, which could be tracked in single  
114 cells by FISH and focal CNAs and SNVs for tracking in single cells by multiplex Q-PCR.  
115 Two DS-ALL patients (19599, 11538) and two non-DS-ALL patients (11543, 21819)  
116 were investigated by single cell multiplex Q-PCR(23). SVs tracked in each patient by  
117 FISH are shown in Supplementary Table 1 and SVs, CNAs and SNVs tracked by Q-PCR  
118 are shown in Supplementary Tables 2 and 3.

### 119 **Xenograft transplants**

120 All *in vivo* studies were performed by personnel holding a current Personal Licence  
121 under the Animals (Scientific Procedures) Act 1986 and were conducted in line with  
122 current Home Office regulations, compliant with the 3R principles (Home Office  
123 license number PPL 60/4552). No further ethical approval was required. Animals were  
124 housed under pathogen free conditions, and all experimental manipulations were  
125 performed on anaesthetized mice under sterile conditions in a laminar flow hood.

126 Male and female NSG mice (Jax<sup>®</sup> mice strain name: NOD.Cg-Prkdcscid Il2rgtm1wjl/SzJ)  
127 were transplanted with  $1 \times 10^6$  patient primary bone marrow cells, injected  
128 intrafemorally into the right femur, as previously described (27). Animals were  
129 maintained until they showed clinical signs (weight loss, palpable spleen), which  
130 necessitated humane killing (range 3-10 months post injection). Patient-derived  
131 xenograft cells (PDXs) from the bone marrow and spleen were harvested, passed  
132 through cell strainers (0.40 $\mu$ m) and frozen for long term storage in 90% foetal calf  
133 serum and 10% DMSO in liquid nitrogen.

#### 134 **Cytogenetics and fluorescence in situ hybridisation**

135 Fixed cells were available for 47 *CRLF2*-r patients (46 at diagnosis and 1 at relapse): 14  
136 patients were DS (*P2RY8-CRLF2*, n=12; *IGH-CRLF2*, n=2) and 33 were non-DS (*P2RY8-*  
137 *CRLF2*, n=25; *IGH-CRLF2*, n=8) (Supplementary Table 1). Where possible, direct fixed  
138 cell cultures were tested to prevent discrepancies caused by outgrowth of normal cells  
139 and death of malignant cells. Multiple colour interphase FISH was used to assess the  
140 simultaneous presence of both *CRLF2*-r (XX-87136C11, XX-82904A1, RP4-674K4, RP11-  
141 309C18)(10) and deletions of *CDKN2A/B* (RP11-149I2) and/or *PAX5* (RP11-469D03)  
142 and/or *IKZF1* (G248P800745C8/WI2-3001F15) (previously identified by MLPA and  
143 single nucleotide polymorphism (SNP) arrays (26)) in the same cell, as previously

144 reported (10, 28). Briefly, home-grown FISH probes were mixed 1:1 with hybridisation  
145 buffer (company) and denatured at 75°C for five minutes followed by hybridisation at  
146 37°C overnight. Coverslips were removed in 2x SSC and slides washed in 0.02% SSC  
147 with 0.003% NP40 at 72°C for two minutes followed incubation in 0.1% SSC at room  
148 temperature for two minutes. Slides were mounted with 10ul DAPI (Vector  
149 laboratories, California, USA). Automated capture and scoring was performed using  
150 an automated Olympus BX-61 8-bay stage fluorescence microscope with a x60 oil  
151 objective. Images were stored and analysed using the CytoVision 7.2 SPOT counting  
152 system (Leica Microsystems, Gateshead, UK). Where possible, more than 100 nuclei  
153 were scored for each FISH test by two independent analysts. A cut-off threshold of  
154 >8% was used for all multiple colour probe combinations to allow for interference and  
155 obscuring of signals. The cut-off level was established by counting the number of  
156 abnormal (false positive) signals generated when the multiple colour probe  
157 combinations were hybridised to normal cells.

#### 158 **Commercial and custom primers for Q-PCR and digital PCR**

159 We aimed to track all identified somatic SVs and SNVs detected by WGS and WES  
160 encompassing those present at high and low variant allele frequencies; some could  
161 not be tracked due to the sequence surrounding the rearrangement (Supplementary  
162 Tables 2 and 3).

163 Custom Taqman Q-PCR assays for SV or SNP that could distinguish the mutant allele  
164 from its wild-type counterpart were designed as previously described (23). DNA copy  
165 number Taqman assays were purchased from Applied Biosystems. Three CNA assays  
166 were chosen within each DNA target region of interest and the diploid reference  
167 region encompassing *B2M* (Supplementary Table 4).

168 **FACS for single cell collection**

169 Diagnostic patient samples and those previously harvested from xenograft transplants  
170 were thawed from liquid nitrogen and bulk cells were labelled with carboxyfluorescein  
171 diacetate, succinimidyl ester (CFSE) and 6 diamidino-2-phenylindole (DAPI) to identify  
172 live and dead cells, respectively. Cells retrieved from successful transplantations into  
173 NSG mice were also labelled with phycoerythrin (PE)–conjugated anti-human CD45  
174 and allophycocyanin (APC)–conjugated anti-mouse CD45 antibodies (BD Biosciences)  
175 before resuspension in PBS and DAPI in order to identify and sort the human  
176 leukaemic cells.

177 **Single Cell Sorting and multiplex Q-PCR analysis**

178 Single cell sorting was carried out after staining, according to our established protocol,  
179 as previously described (23). Briefly, single cells were sorted from each case into  
180 individual wells of a 96 well plate and lysed. The DNA target region of interest,  
181 including patient specific gene fusions, SNVs and CNAs, was amplified. We collected  
182 252-336 cells from the diagnostic ALL samples, 81-252 cells from PDX and 48 cord  
183 blood cells (normal diploid control). A cell was called positive for a SNP (or SNV) if the  
184 Q-PCR cycle threshold ( $C_T$ ) value was below 28. We used a modified version of the  
185  $\Delta\Delta C_T$  method (Applied Biosystems, Life Technologies Ltd.) to integrate results from  
186 multiple Taqman assays targeting the same region to determine the relative copy  
187 number for each locus. The use of multiple assays to target one region increased the  
188 accuracy of attributed CNAs. The resulting reaction mix was then diluted and Q-PCR  
189 completed using the 96x96 dynamic array and the BioMark™ HD from Fluidigm.  
190 Several approaches were adopted during this experiment to optimise and confirm the  
191 presence of single cells and ensure that all assays performed efficiently under



192 experimental conditions (23). Assay error rates in these experiments were zero. Single  
193 cell data removed from the Q-PCR analysis included those from wells with no data (no  
194 cell) and those wells in which all *B2M* assays did not have a strong signal (<25 C<sub>T</sub>). On  
195 average this accounted for the removal of ~9% of data points. Only mutational spectra  
196 occurring in more than one cell were included in the analysis.

## 197 **Results**

198 To explore whether *IGH-CRLF2* and *P2RY8-CRLF2* were early or late events in the  
199 evolution of B-ALL, we performed multiple colour FISH on 47 ALL patient samples to  
200 track the *CRLF2-r* (*IGH-CRLF2*, n=10, *P2RY8-CRLF2*, n=37) and deletions common in  
201 ALL: *IKZF1* and/or *CDKN2A/B* and/or *PAX5*.

### 202 *IGH-CRLF2* is an early event in B-ALL

203 In those patients with *IGH-CRLF2* bone marrow blast counts at diagnosis correlated  
204 with the percentage of abnormal blasts detected by multiple colour FISH  
205 (Supplementary Table 1), suggesting that the tracked abnormalities were present in  
206 the major leukaemic clone. In 80% (8/10), *IGH-CRLF2* was a clonal event, either  
207 presenting first in the majority of cells in four patients, or together with other tracked  
208 abnormalities in four patients (examples of FISH signal patterns are shown in Figures  
209 1A and 1B).

### 210 *P2RY8-CRLF2* is an early event in B-ALL

211 In 73% (27/37) of patients with *P2RY8-CRLF2*, the bone marrow blast counts at  
212 diagnosis correlated with the percentage of abnormal blasts detected by multiple  
213 colour FISH (Supplementary Table 1). *P2RY8-CRLF2* presented as the first tracked  
214 abnormality in 9/27 patients and together with other abnormalities in 18/27 patients  
215 (for one case only relapse material was available; 6897) (examples of FISH signal

216 patterns are shown in Figures 1C and 1D).

217 *CRLF2-r* are observed as sub-clonal events in B-ALL

218 While most patients with *IGH-CRLF2* have the rearrangement as an early event in  
219 leukaemogenesis, in two *IGH-CRLF2* patients (3789 and 3141), loss of *IKZF1* was  
220 detected as the earliest event with *IGH-CRLF2* observed only in a sub-clone (example  
221 from patient 3789 is shown in Figure 2A). Patient 3141 had two subsequent relapses;  
222 at second relapse, the *IKZF1* deletion was present in 64% of cells compared to 33% for  
223 *IGH-CRLF2* as assessed by individual FISH tests (data not shown). These data confirm  
224 the sub-clonal nature of *IGH-CRLF2* in this patient.

225 Similarly, the sub-clonal nature of *P2RY8-CRLF2* was observed in 24% (9/37) of the  
226 patients, where the percentage of abnormal cells detected by FISH was notably less  
227 than the blast count at diagnosis, suggesting that the earliest events remained  
228 undetected in these patients (Supplementary Table 1). Of particular interest was  
229 patient 2017, where monoallelic loss of *CDKN2A/B* and *PAX5* preceded the formation  
230 of the fusion (Figure 2B). Of the two or three abnormalities tracked by FISH, *P2RY8-*  
231 *CRLF2* presented first in 4/9 patients and together with other abnormalities in 5/9  
232 patients.

233 Parallel evolution occurs in the development of *CRLF2-r* ALL

234 In five *P2RY8-CRLF2* patients, evidence of parallel evolution of cells containing  
235 abnormalities of one or more genes was observed (Figure 3A-E). In three patients  
236 (12200, 3173, 4954), four sub-clones were identified. In patients 12200 and 3173,  
237 (Figure 3A and B, respectively), clones harbouring either the *P2RY8-CRLF2* fusion or  
238 loss of *CDKN2A/B* or *IKZF1*, respectively, occurred in sub-clones. The main clone seen  
239 at diagnosis must have evolved from a cell that acquired both abnormalities giving it

240 a competitive advantage over the other sub-clone. In patient 4954 (Figure 3C), the  
241 *P2RY8-CRLF2* fusion was present together with either, loss of one or two copies of  
242 *CDKN2A/B* and loss of one copy of *IKZF1*. These data suggest that *CDKN2A/B*  
243 undergoes deletions in independent sub-clones. The main clone seen at diagnosis  
244 must have evolved from a cell that acquired all three abnormalities giving it a  
245 competitive advantage over the other sub-clone.

246 In patients 20753 and 5817, the parallel clones were defined by the *CRLF2-r*. In patient  
247 20753 (Figure 3D), one sub-clone gained an extra *P2RY8-CRLF2* fusion with subsequent  
248 loss of a single copy of *PAX5* prior to the loss of the second copy of *IKZF1*. In patient  
249 5817 (Figure 3E), the sub-clones harboured either a *CRLF2-r* with loss of one copy of  
250 *IKZF1* (9%) or *P2RY8-CRLF2* alone (17%). Identical parallel evolution was found in  
251 patient 21572 (Figure 3F). The parallel clones were defined by an *IGH-CRLF2*  
252 translocation alone or a *CRLF2-r* coupled with loss of one copy of *IKZF1*. Together these  
253 data suggest the sub-clonal architecture observed in these cases could only have  
254 occurred if *IKZF1* and/or *CDKN2A/B* undergo deletions in independent sub-clones.

255 Single cell multiplex Q-PCR identified linear and branching development of *CRLF2-r*

256 ALL

257 Whilst FISH allowed the detection of a small number of large SVs, it was not possible  
258 to investigate associations between small CNAs and SNVs. Single cell multiplex Q-PCR  
259 allowed a more comprehensive analysis of four patients. Individual cells were sorted  
260 from the leukaemia sample and assayed by multiplex Q-PCR for the presence of  
261 specific genetic aberrations previously identified from WGS and WES (26). A similar  
262 assessment was carried out using unsorted PDX ALL cells from the same patients in  
263 order to determine self-renewal properties of discrete clones. From these samples

264 and expanded single cell data, we were able to define detailed clonal architectures in  
265 which genetically distinct sub-clones were characterised by SVs, SNVs and CNAs  
266 (Figure 4).

267 In non-DS-ALL patients 11543 and 21819 a linear architecture was observed (Figure  
268 4A and B). In patient 11543 (Figure 4A) the *IGH-CRLF2* translocation was secondary to  
269 multiple CNAs and SNVs, including an initial *IKZF1* deletion, with a second *IKZF1*  
270 deletion occurring after the acquisition of the *IGH-CRLF2* translocation. The  
271 architecture was recapitulated in both xenograft bone marrow and spleen cells,  
272 suggesting that all sub-clones possessed self-renewal properties. In patient 21819  
273 (Figure 4B) the *P2RY8-CRLF2* fusion was secondary to loss of *IKZF1* and *CDKN2A* (Figure  
274 4C). Serial xenograft transplants were ultimately populated by the major *P2RY8-CRLF2*  
275 containing clone seen at diagnosis.

276 In contrast, the two DS-ALL patients, 19599 and 11538, showed a branching sub-clonal  
277 architecture where the *CRLF2-r* was one of several structural alterations that defined  
278 the earliest identified clone (Figure 4C and D). In patient 19599 (Figure 4C) the sub-  
279 clonal architecture was defined by discrete *IKZF1* and *JAK2* mutations. A single evolved  
280 clone from the diagnostic sample engrafted into both spleen and bone marrow of  
281 transplanted mice, suggesting that the other sub-clones had a reduced self-renewal  
282 ability. In patient 11538 (Figure 4D) the sub-clonal architecture was defined by  
283 multiple *IKZF1* events and additional mutations that were secondary to the *P2RY8-*  
284 *CRLF2* fusion. Whilst the architecture was recapitulated in the xenograft, the major  
285 clones at diagnosis were present as minor clones in the xenografts.

286 Whilst multiple mice were not analysed by single cell QPCR for each sample, FISH was  
287 completed and showed comparable results (data not shown).

288

289 **Discussion**

290 In several blood cell cancers there appears to be a preferential order of mutations,  
291 including in ALL (20, 21, 29, 30), AML (31) and MDS (32-34). To determine whether  
292 *IGH-CRLF2* and *P2RY8-CRLF2* were early or late events in the evolution of B-ALL, we  
293 carried out single cell analysis using both FISH and multiplex Q-PCR of 51 DS and non-  
294 DS-ALL patients. Forty-seven were investigated by FISH for specific rearrangements  
295 including *P2RY8-CRLF2* or *IGH-CRLF2* coupled with deletions of *IKZF1*, *PAX5* or  
296 *CDKN2A/B*. The remaining four cases underwent a more detailed analysis using  
297 multiplex Q-PCR for multiple patient specific SVs, SNVs and CNAs.

298 *CRLF2-r* were observed as common early events in the majority of patients studied,  
299 including DS and non-DS-ALL patients. However, the *P2RY8-CRLF2* fusion was also  
300 found to be sub-clonal in approximately one quarter of patients investigated. The sub-  
301 clonal nature of the *P2RY8-CRLF2* fusion has previously been reported (17). In  
302 contrast, the early nature of both *IGH-CRLF2* and *P2RY8-CRLF2* in DS-ALL was recently  
303 reported, where 92% (11/12) of patients retained these rearrangements at relapse.  
304 The authors suggested that both rearrangements were early events in  
305 leukaemogenesis which may play important roles at relapse (18). However, other  
306 evidence suggests that relapse in ALL can originate from sub-clones distributed  
307 anywhere in the phylogenetic architecture of the cancer (20, 35-37), indicating that  
308 the preservation of any individual genetic lesion in relapse does not necessarily reflect  
309 a founder , early or truncal status.

310 In the present study, six patients showed the potential development of two  
311 independent leukaemias with clones showing parallel evolution driven by reiterative

312 CNAs within the same genes. In three patients with *P2RY8-CRLF2* loss of one copy of  
313 the other tracked gene occurred in discrete populations. The bulk of the leukaemia  
314 then evolved from a cell acquiring both abnormalities. In the remaining three patients  
315 the parallel clones were defined by distinct early *CRLF2-r*. The presence of reiterative  
316 genetic changes has been reported in ALL before (20, 38) and they are thought to arise  
317 by RAG-mediated mutagenesis (22). Reiterative mutation is a relatively common  
318 feature in other cancers (39) reflecting convergent (or parallel) evolution in the  
319 context of common selective pressures. It is also important to consider that we are  
320 analysing one sample at a single time point in the development of this disease. It is  
321 not always possible to determine the precise temporal order in which events take  
322 place during tumour development unless representative populations of all ancestral  
323 clones remain at diagnosis. In those where we observed the *CRLF2-r* and deletions of  
324 other genes as the earliest identifiable events, it is possible that they arose  
325 sequentially with the earliest events no longer being present at diagnosis. The limited  
326 sensitivity of FISH for detecting these rare clones impacts how precise we can be in  
327 mapping the temporal order of tumour development.

328 Sub-clonal heterogeneity and clonal selection has been studied in many  
329 haematological diseases, highlighting the importance of understanding sub-clonal  
330 architecture in relation to therapeutic decisions regarding individual patients (38, 40,  
331 41). Single cell multiplex Q-PCR in two DS-ALL patients revealed the presence of *IGH-*  
332 *CRLF2* or *P2RY8-CRLF2* in the earliest clone, together with a multitude of SNVs and  
333 other CNAs. These patients showed a complex branching tree structure with  
334 reiterative deletions and mutations occurring in different sub-clonal populations. In  
335 contrast, the leukaemia in the two non-DS-ALL patients appeared to evolve in a linear

336 non-branching manner with *IGH-CRLF2* or *P2RY8-CRLF2* occurring on a background of  
337 SNVs or CNAs and arising later in leukaemia development. These data suggest that  
338 *IGH-CRLF2* and *P2RY8-CRLF2* could be earlier events in DS-ALL compared to non-DS-  
339 ALL. Although our results suggest that there is no difference between DS and non-DS  
340 ALL, we are - despite simultaneously tracking several alterations - still likely  
341 underestimating the complexity of clonal phylogeny.

342 The application of single cell Q-PCR to PDX cells demonstrated that in three of the four  
343 patients, the majority of clones identified at diagnosis had leukaemia propagating  
344 capacity, being present in both bone marrow and spleen in primary and second  
345 generation mice. In the PDX cells from patient 19599, only one sub-clone engrafted,  
346 suggesting that either the other sub-clones did not have self-propagating capacity, or  
347 that they were below the level of detection within the diagnostic sample. Such findings  
348 have been previously reported, in which analysis of CNAs from mice injected with as  
349 few as 100 cells remained highly related to the diagnostic sample, with only a few  
350 novel deletions arising in the primary mice (42). In some samples, clonal outgrowth of  
351 the dominant diagnostic clone was observed; however, in others they observed  
352 outgrowth of sub-clones (42). The outgrowth of certain clones would not necessarily  
353 mean the clones that are no longer present are incapable of self-renewal, but are less  
354 suited to the murine environment.

355 Evolution of cancer was initially assumed to be driven by a steady accumulation of  
356 genomic abnormalities over time. However, others have suggested that the presence  
357 of explosive changes caused by global genomic instability (43), a chromothripsis event  
358 (44) or the effect of a single high impact mutation (45, 46) may be responsible.

359 Previous work has postulated that additional copies of chromosome 21 can promote

360 genomic instability (47, 48). Interestingly, among the four patients studied here by  
361 multiplex Q-PCR, three showed a large number of abnormalities in the earliest clone  
362 (range 11-20), suggesting that either a single or series of explosive events may have  
363 occurred creating a backbone of aberrations upon which further evolution could take  
364 place. Notably these three patients had either constitutional or somatic gain of  
365 chromosome 21 either.

366 In summary, our data indicates that *CRLF2-r* co-operate with multiple additional  
367 genetic alterations in ALL and that there appears to be no major restraint on whether  
368 *CRLF2-r* arise early as a founder or truncal event or later in clonal evolution.

369

#### 370 **Acknowledgements**

371 The authors would like to thank The Kay Kendall Leukaemia Fund, Leuka, Children with  
372 Cancer UK and Bloodwise (formerly Leukaemia and Lymphoma Research) for financial  
373 support. Lisa J Russell has a John Goldman Fellowship from Leuka. We also thank  
374 member laboratories of the United Kingdom Cancer Cytogenetic Group (UKCCG) for  
375 providing cytogenetic data and material. We are grateful to all the members of the  
376 NCRI Haematological Oncology Adult ALL Subgroup and the NCRI Childhood Cancer  
377 and Leukaemia Group (CCLG) Leukaemia Subgroup. Primary childhood leukaemia  
378 samples used in this study were provided by the Bloodwise Childhood Leukaemia Cell  
379 Bank working with the laboratory teams in the Bristol Genetics Laboratory,  
380 Southmead Hospital, Bristol: Molecular Biology Laboratory, Royal Hospital for Sick  
381 Children, Glasgow: Molecular Haematology Laboratory, Royal London Hospital,  
382 London: Molecular Genetics Service and Sheffield Children's Hospital, Sheffield. We  
383 also thank the Central England Haemato-Oncology Research Biobank for providing



384 patient samples. Finally, we thank all the clinicians who entered patients into the trial  
385 and the patients and families who agreed to take part.

386

### 387 **Competing interests**

388 All authors have no conflicts of interest to disclose

389

### 390 **Data availability**

391 Data sharing not applicable to this article as no datasets were generated or analysed  
392 during the current study.

393

### 394 **References**

- 395 1. Moorman AV. The clinical relevance of chromosomal and genomic abnormalities in  
396 B-cell precursor acute lymphoblastic leukaemia. *Blood Reviews*. 2012;26(3):123-35.
- 397 2. Wiemels JL, Cazzaniga G, Daniotti M, Eden OB, Addison GM, Masera G, et al.  
398 Prenatal origin of acute lymphoblastic leukaemia in children. *The Lancet*.  
399 1999;354(9189):1499-503.
- 400 3. Greaves MF, Maia AT, Wiemels JL, Ford AM. Leukemia in twins: lessons in natural  
401 history. *Blood*. 2003;102(7):2321-33.
- 402 4. Maia AT, van der Velden VHJ, Harrison CJ, Szczepanski T, Williams MD, Griffiths  
403 MJ, et al. Prenatal origin of hyperdiploid acute lymphoblastic leukemia in identical twins.  
404 *Leukemia*. 2003;17(11):2202-6.
- 405 5. Mori H, Colman SM, Xiao Z, Ford AM, Healy LE, Donaldson C, et al. Chromosome  
406 translocations and covert leukemic clones are generated during normal fetal development.  
407 *Proceedings of the National Academy of Sciences of the United States of America*.  
408 2002;99(12):8242-7.
- 409 6. Wiemels JL, Ford AM, Van Wering ER, Postma A, Greaves M. Protracted and  
410 Variable Latency of Acute Lymphoblastic Leukemia After TEL-AML1 Gene Fusion In Utero.  
411 *Blood*. 1999;94(3):1057-62.
- 412 7. Den Boer ML, van Slegtenhorst M, De Menezes RX, Cheok MH, Buijs-Gladdines JG,  
413 Peters ST, et al. A subtype of childhood acute lymphoblastic leukaemia with poor treatment  
414 outcome: a genome-wide classification study. *The Lancet Oncology*. 2009;10(2):125-34.
- 415 8. Mullighan CG, Su X, Zhang J, Radtke I, Phillips LAA, Miller CB, et al. Deletion of  
416 IKZF1 and Prognosis in Acute Lymphoblastic Leukemia. *New England Journal of Medicine*.  
417 2009;360(5):470-80.
- 418 9. Roberts KG, Li Y, Payne-Turner D, Harvey RC, Yang YL, Pei D, et al. Targetable  
419 kinase-activating lesions in Ph-like acute lymphoblastic leukemia. *New England Journal of*  
420 *Medicine*. 2014;371(11):1005-15.
- 421 10. Russell LJ, Capasso M, Vater I, Akasaka T, Bernard OA, Calasanz MJ, et al.  
422 Deregulated expression of cytokine receptor gene, CRLF2, is involved in lymphoid

423 transformation in B-cell precursor acute lymphoblastic leukemia. *Blood*. 2009;114(13):2688-  
424 98.

425 11. Mullighan CG, Collins-Underwood JR, Phillips LA, Loudin MG, Liu W, Zhang J, et al.  
426 Rearrangement of CRLF2 in B-progenitor- and Down syndrome-associated acute  
427 lymphoblastic leukemia. *Nat Genet*. 2009;41(11):1243-6.

428 12. Chapiro E, Russell L, Lainey E, Kaltenbach S, Ragu C, Della-Valle V, et al. Activating  
429 mutation in the TSLPR gene in B-cell precursor lymphoblastic leukemia. *Leukemia*.  
430 2010;24(3):642-5.

431 13. Moorman AV, Schwab C, Ensor HM, Russell LJ, Morrison H, Jones L, et al. IGH@  
432 Translocations, CRLF2 Dereglulation, and Microdeletions in Adolescents and Adults With  
433 Acute Lymphoblastic Leukemia. *Journal of Clinical Oncology*. 2012;30(25):3100-8.

434 14. Schwab CJ, Jones LR, Morrison H, Ryan SL, Yigittop H, Schouten JP, et al. Evaluation  
435 of multiplex ligation-dependent probe amplification as a method for the detection of copy  
436 number abnormalities in B-cell precursor acute lymphoblastic leukemia. *Genes Chromosomes  
437 Cancer*. 2010;49(12):1104-13.

438 15. Buitenkamp TD, Pieters R, Gallimore NE, van der Veer A, Meijerink JPP, Beverloo  
439 HB, et al. Outcome in children with Down's syndrome and acute lymphoblastic leukemia: role  
440 of IKZF1 deletions and CRLF2 aberrations. *Leukemia*. 2012;26(10):2204-11.

441 16. Roberts KG, Morin RD, Zhang J, Hirst M, Zhao Y, Su X, et al. Genetic alterations  
442 activating kinase and cytokine receptor signaling in high-risk acute lymphoblastic leukemia.  
443 *Cancer Cell*. 2012;22(2):153-66.

444 17. Morak M, Attarbaschi A, Fischer S, Nassimbeni C, Grausenburger R, Bastelberger S,  
445 et al. Small sizes and indolent evolutionary dynamics challenge the potential role of P2RY8-  
446 CRLF2-harboring clones as main relapse-driving force in childhood ALL. *Blood*.  
447 2012;120(26):5134-42.

448 18. Schwartzman O, Savino AM, Gombert M, Palmi C, Cario G, Schrappe M, et al.  
449 Suppressors and activators of JAK-STAT signaling at diagnosis and relapse of acute  
450 lymphoblastic leukemia in Down syndrome. *Proceedings of the National Academy of Sciences*.  
451 2017;114(20):E4030-E9.

452 19. Wolman SR. Cytogenetic heterogeneity: its role in tumor evolution. *Cancer Genet  
453 Cytogenet*. 1986;19(1-2):129-40.

454 20. Anderson K, Lutz C, van Delft FW, Bateman CM, Guo Y, Colman SM, et al. Genetic  
455 variegation of clonal architecture and propagating cells in leukaemia. *Nature*.  
456 2011;469(7330):356-61.

457 21. Ma X, Edmonson M, Yergeau D, Muzny DM, Hampton OA, Rusch M, et al. Rise and  
458 fall of subclones from diagnosis to relapse in pediatric B-acute lymphoblastic leukaemia.  
459 *Nature communications*. 2015;6:6604.

460 22. Papaemmanuil E, Rapado I, Li Y, Potter NE, Wedge DC, Tubio J, et al. RAG-mediated  
461 recombination is the predominant driver of oncogenic rearrangement in ETV6-RUNX1 acute  
462 lymphoblastic leukemia. *Nat Genet*. 2014;46(2):116-25.

463 23. Potter NE, Ermini L, Papaemmanuil E, Cazzaniga G, Vijayaraghavan G, Titley I, et al.  
464 Single-cell mutational profiling and clonal phylogeny in cancer. *Genome Research*.  
465 2013;23(12):2115-25.

466 24. Navin N, Kendall J, Troge J, Andrews P, Rodgers L, McIndoo J, et al. Tumour  
467 evolution inferred by single-cell sequencing. *Nature*. 2011;472(7341):90-4.

468 25. Gerlinger M, Rowan AJ, Horswell S, Math M, Larkin J, Endesfelder D, et al.  
469 Intratumor heterogeneity and branched evolution revealed by multiregion sequencing. *New  
470 England Journal of Medicine*. 2012;366(10):883-92.

471 26. Russell LJ, Jones L, Enshaei A, Tonin S, Ryan SL, Eswaran J, et al. Characterisation  
472 of the genomic landscape of CRLF2-rearranged acute lymphoblastic leukemia.  
473 2017;56(5):363-72.

474 27. le Viseur C, Hotfilder M, Bomken S, Wilson K, Rottgers S, Schrauder A, et al. In  
475 childhood acute lymphoblastic leukemia, blasts at different stages of immunophenotypic  
476 maturation have stem cell properties. *Cancer Cell*. 2008;14(1):47-58.

477 28. Jeffries SJ, Jones L, Harrison CJ, Russell LJ. IGH@ translocations co-exist with other  
478 primary rearrangements in B-cell precursor acute lymphoblastic leukemia. *Haematologica*.  
479 2014;99(8):1334-42.

480 29. Furness CL, Mansur MB, Weston VJ, Ermini L, van Delft FW, Jenkinson S, et al. The  
481 subclonal complexity of STIL-TAL1+ T-cell acute lymphoblastic leukaemia. *Leukemia*. 2018.

482 30. De Bie J, Demeyer S, Alberti-Servera L, Geerdens E, Segers H, Broux M, et al. Single-  
483 cell sequencing reveals the origin and the order of mutation acquisition in T-cell acute  
484 lymphoblastic leukemia. *Leukemia*. 2018.

485 31. Shlush LI, Zandi S, Mitchell A, Chen WC, Brandwein JM, Gupta V, et al. Identification  
486 of pre-leukaemic haematopoietic stem cells in acute leukaemia. *Nature*. 2014;506(7488):328-  
487 33.

488 32. Dussiau C, Fontenay M. Mechanisms underlying the heterogeneity of myelodysplastic  
489 syndromes. *Exp Hematol*. 2018;58:17-26.

490 33. Kim T, Tyndel MS, Kim HJ, Ahn JS, Choi SH, Park HJ, et al. The clonal origins of  
491 leukemic progression of myelodysplasia. *Leukemia*. 2017;31(9):1928-35.

492 34. Kent DG, Ortmann CA, Green AR. Effect of mutation order on myeloproliferative  
493 neoplasms. *The New England journal of medicine*. 2015;372(19):1865-6.

494 35. Mullighan CG, Phillips LA, Su X, Ma J, Miller CB, Shurtleff SA, et al. Genomic  
495 analysis of the clonal origins of relapsed acute lymphoblastic leukemia. *Science*.  
496 2008;322(5906):1377-80.

497 36. van Delft FW, Horsley S, Colman S, Anderson K, Bateman C, Kempinski H, et al. Clonal  
498 origins of relapse in ETV6-RUNX1 acute lymphoblastic leukemia. *Blood*. 2011;117(23):6247-  
499 54.

500 37. Ford AM, Mansur MB, Furness CL, van Delft FW, Okamura J, Suzuki T, et al.  
501 Protracted dormancy of pre-leukemic stem cells. *Leukemia*. 2015;29(11):2202-7.

502 38. Melchor L, Brioli A, Wardell CP, Murison A, Potter NE, Kaiser MF, et al. Single-cell  
503 genetic analysis reveals the composition of initiating clones and phylogenetic patterns of  
504 branching and parallel evolution in myeloma. *Leukemia*. 2014;28(8):1705-15.

505 39. Gerlinger M, Horswell S, Larkin J, Rowan AJ, Salm MP, Varela I, et al. Genomic  
506 architecture and evolution of clear cell renal cell carcinomas defined by multiregion  
507 sequencing. *Nat Genet*. 2014;46(3):225-33.

508 40. Davies NJ, Kwok M, Gould C, Oldreive CE, Mao J, Parry H, et al. Dynamic changes  
509 in clonal cytogenetic architecture during progression of chronic lymphocytic leukemia in  
510 patients and patient-derived murine xenografts. *Oncotarget*. 2017;8(27):44749-60.

511 41. Belderbos ME, Koster T, Ausema B, Jacobs S, Sowdagar S, Zwart E, et al. Clonal  
512 selection and asymmetric distribution of human leukemia in murine xenografts revealed by  
513 cellular barcoding. *Blood*. 2017;129(24):3210-20.

514 42. Schmitz M, Breithaupt P, Scheidegger N, Cario G, Bonapace L, Meissner B, et al.  
515 Xenografts of highly resistant leukemia recapitulate the clonal composition of the  
516 leukemogenic compartment. *Blood*. 2011;118(7):1854-64.

517 43. Shlien A, Campbell BB, de Borja R, Alexandrov LB, Merico D, Wedge D, et al.  
518 Combined hereditary and somatic mutations of replication error repair genes result in rapid  
519 onset of ultra-hypermutated cancers. *Nat Genet*. 2015;47(3):257-62.

520 44. Stephens PJ, Greenman CD, Fu B, Yang F, Bignell GR, Mudie LJ, et al. Massive  
521 genomic rearrangement acquired in a single catastrophic event during cancer development.  
522 *Cell*. 2011;144(1):27-40.

523 45. Hart JR, Zhang Y, Liao L, Ueno L, Du L, Jonkers M, et al. The butterfly effect in  
524 cancer: a single base mutation can remodel the cell. *Proceedings of the National Academy of  
525 Sciences of the United States of America*. 2015;112(4):1131-6.

526 46. Lee RS, Stewart C, Carter SL, Ambrogio L, Cibulskis K, Sougnez C, et al. A  
527 remarkably simple genome underlies highly malignant pediatric rhabdoid cancers. *J Clin  
528 Invest*. 2012;122(8):2983-8.

529 47. Cabelof DC, Patel HV, Chen Q, van Remmen H, Matherly LH, Ge Y, et al. Mutational  
530 spectrum at GATA1 provides insights into mutagenesis and leukemogenesis in Down  
531 syndrome. *Blood*. 2009;114(13):2753-63.

532 48. Hertzberg L, Vendramini E, Ganmore I, Cazzaniga G, Schmitz M, Chalker J, et al.  
533 Down syndrome acute lymphoblastic leukemia, a highly heterogeneous disease in which  
534 aberrant expression of CRLF2 is associated with mutated JAK2: a report from the International  
535 BFM Study Group. *Blood*.115(5):1006-17.  
536  
537

538 **Figure Legends**

539 **Figure 1. Multiple colour FISH showing examples of *IGH-CRLF2* as a clonal event**  
540 **arising (A) first or (B) together with other tracked abnormalities (C) *P2RY8-CRLF2* as**  
541 **a clonal event arising first or (D) together with other tracked abnormalities.**

- 542 • Representative FISH images on the right show examples of each leukaemic  
543 sub-clone.
- 544 • Leukaemic sub-clone percentages for the diagnostic samples are indicated  
545 next to each clone and only include populations above the 8% cut off.
- 546 • Dotted clone with “?”: presumed but undetected founder clone.

547 **(A) For patient 23394** a total of 245 abnormal nuclei at diagnosis were scored for  
548 probes to *CRLF2* (red/green) and *CDKN2A/B* (gold). In 34% of nuclei the *IGH-CRLF2*  
549 translocations was an early event observed in the presence of two copies of  
550 *CDKN2A/B*. This clone evolves into two sub-clones: one gains an extra copy of *IGH* in  
551 17% of nuclei; one loses a single copy of *CDKN2A/B* in 49% of nuclei.

552 **(B) For patient 4001** a total of 129 abnormal nuclei at diagnosis were scored for probes  
553 to *CRLF2* (red/green), *IKZF1* (gold) and *PAX5* (aqua). In 67% of nuclei the *IGH-CRLF2*  
554 translocation was present with one copy of *IKZF1* and two copies of *PAX5*. This clone  
555 evolves with loss of a single copy of *PAX5* in 33% of nuclei.

556 **(C) For patient 10924** a total of 227 abnormal nuclei at diagnosis were scored for  
557 probes to *CRLF2* (red/green) and *IKZF1* (gold). In 11% of nuclei the *P2RY8-CRLF2* fusion  
558 is an early event before the loss of a single copy of *IKZF1* observed in the bulk  
559 leukaemic clone at 89%.

560 **(D) For patient 322** a total of 70 abnormal nuclei at diagnosis were scored for probes  
561 to *CRLF2* (red/green) and *CDKN2A/B* (gold). In 67% of nuclei the *P2RY8-CRLF2* fusion

562 and loss of a single copy of *CDKN2A/B* present together. A further 33% of cells gained  
563 an additional copy of the *CRLF2* probe, which usually indicates the presence of an  
564 additional sex chromosome (+X/Y).

565

566

567

568

569

570

571

572

573

574

575

576

577

578

579

580

581

582

583

584

585 **Figure 2. Multiple colour FISH showing examples of the sub-clonal nature of (A)**

586 ***P2RY8-CRLF2* (B) *IGH-CRLF2***

587 • Representative FISH images on the right show examples of each leukaemic  
588 sub-clone.

589 • DAPI has been removed from panel B in order for the *PAX5* aqua signals to be  
590 observed.

591 • Leukaemic sub-clone percentages for the diagnostic samples are indicated  
592 next to each clone and only include populations above the 8% cut off.

593 • Dotted clone with “?”: presumed but undetected founder clone.

594 **(A) For patient 3789** a total of 144 abnormal nuclei at diagnosis were scored for probes  
595 to *CRLF2* (red/green) and *IKZF1* (gold). In 11% of nuclei both copies of *IKZF1* are  
596 deleted. This clone subsequently acquires the *IGH-CRLF2* translocation in a further  
597 83% of cells.

598 **(B) For patient 2017** a total of 211 abnormal nuclei at diagnosis were scored for probes  
599 to *CRLF2* (red/green) and *CDKN2A/B* (gold) and *PAX5* (aqua). The earliest abnormal  
600 clone detected has loss of a single copy of *CDK2NA/B* and *PAX5* suggesting *P2RY8-*  
601 *CRLF2* is a sub-clonal event. This clone acquired *P2RY8-CRLF2* in a further 70% of  
602 nuclei.

603

604

605

606

607

608

609 **Figure 3. Multiple colour FISH showing examples of parallel evolution in (A-E) *P2RY8-***  
610 ***CRLF2* (F) *IGH-CRLF2* patients driven by reiterative CNAs within the same genes**

- 611 • Leukaemic sub-clone percentages for the diagnostic samples are indicated  
612 next to each clone and only include sub-clones above the 8% cut off.
- 613 • Dashed lines present possible alternate routes to final sub-clone. It is likely that  
614 one sub-clone was not competitive enough and the other acquired the  
615 additional abnormality to continue evolving.
- 616 • Dotted clone with “?”: presumed but undetected founder clone.

617 **(A) For patient 12200** a total of 269 abnormal nuclei at diagnosis were scored for  
618 probes to *CRLF2* and *CDKN2A/B*. Two independent clones evolved from an  
619 undetectable founder clone either losing both copies of *CDKN2A/B* in 19% or acquiring  
620 the *P2RY8-CRLF2* fusion in 16%. The major clone encompassing 65% of nuclei was  
621 observed to have both abnormalities from the previous two independent clones with  
622 an additional copy of *CRLF2*, which usually indicates the presence of an additional sex  
623 chromosome.

624 **(B) For patient 3173** a total of 58 abnormal nuclei at diagnosis were scored for probes  
625 to *CRLF2* and *IKZF1*. Two independent clones evolved from an undetectable founder  
626 clone either losing a single copy of *IKZF1* in 10% or the formation of *P2RY8-CRLF2* in  
627 45%. A clone was observed to have evolved from either previous clone by gaining the  
628 *P2RY8-CRLF2* fusion or losing a single copy of *IKZF1*, respectively.

629 **(C) For patient 4954** a total of 50 abnormal nuclei at diagnosis were scored for probes  
630 to *CRLF2*, *IKZF1* and *CDKN2A/B*. The earliest clone detected harboured the *P2RY8-*  
631 *CRLF2* fusion with loss of a single copy of *CDKN2A/B* in 18%. Two independent clones  
632 evolved from this population either losing a single copy of *IKZF1* in 30% or losing the



633 second copy of *CDKN2A/B* in 20%. The major clone encompassing 32% of nuclei was  
634 observed to have evolved from either previous clone by losing a second copy of  
635 *CDKN2A/B* or losing a single copy of *IKZF1*, respectively.

636 **(D) For patient 20753** a total of 50 abnormal nuclei at diagnosis were scored for  
637 probes to *CRLF2*, *IKZF1* and *PAX5*. The earliest abnormal clone detected harboured the  
638 *P2RY8-CRLF2* fusion with loss of a single copy of *IKZF1* in 18% of nuclei. Two  
639 independent clones evolved from this population either losing the second copy of  
640 *IKZF1* in 18% or doubling up the derived chromosome X to give two copies of *P2RY8-*  
641 *CRLF2* in 20%. This latter clone evolves further to lose a single copy of *PAX5* in 20%  
642 and the second copy of *IKZF1* in a further 24%.

643 **(E) For patient 5817** a total of 120 abnormal nuclei at diagnosis were scored for probes  
644 to *CRLF2* and *IKZF1*. Two independent clones evolved from an undetectable founder  
645 clone. A signal pattern indicative of a rearrangement of *CRLF2* (1R1G1F) in the  
646 presence of a single copy of *IKZF1* was observed in 15% of cells. *P2RY8-CRLF2* alone  
647 (FISH signal pattern 1R0G1F) was observed in an independent clone of 28%. This clone  
648 evolved to lose a single copy of *IKZF1* in 52% followed by doubling up the derived sex  
649 chromosome to give two copies of *P2RY8-CRLF2* in 21%.

650 **(F) For patient 21572** a total of 152 abnormal nuclei at diagnosis were scored for  
651 probes to *CRLF2*, *IKZF1* and *PAX5*. Two independent clones evolved from an  
652 undetectable founder clone with different signal patterns for the *CRLF2*  
653 rearrangements. A signal pattern indicative of a rearrangement of *CRLF2* (1R1G1F)  
654 was observed in 13% of cells in the presence of a single copy of *IKZF1*. *IGH-CRLF2* alone  
655 was observed in an independent clone of 13%. The signal pattern observed in these  
656 cells was 1R0G1F, which in conjunction with a split *IGH* FISH signal pattern, suggests

657 the cells have an *IGH-CRLF2* translocation and a deletion on the derived sex  
658 chromosome involved in the translocation. This clone evolves to lose a single copy of  
659 *IKZF1* in 43% followed by loss of a single copy of *PAX5* in a further 31%.

660

661

662

663

664

665

666

667

668

669

670

671

672

673

674

675

676

677

678

679

680

681 **Figure 4. Sub-clonal architecture demonstrated by single cell analysis**

- 682 • Sub-clone percentages for the diagnostic samples are indicated next to each
- 683 clone.
- 684 • The blue triangle and orange square denote groups of clonal abnormalities
- 685 including SNVs and CNAs.
- 686 • Those sub-clones identified in the primary mouse spleen (S) and bone marrow
- 687 (BM) are indicated using black arrows. Where secondary mice were tested; S-
- 688 S indicates spleen cells and S-BM, bone marrow cells.
- 689 • Where stated, alterations were tracked by either patient specific fusion and
- 690 mutation assays or generic copy number assays.
- 691 • Gene copy numbers, where appropriate are indicated next to the gene name.

692 **(A) Non-DS-ALL patient 11543** - In the diagnostic sample 310 cells were successfully  
693 screened. Bulk diagnostic cells engrafted in three mice, the spleen and bone marrow  
694 (250 cells from each) were investigated from one mouse. At diagnosis the *IGH-CRLF2*  
695 translocation is observed on a background of clonal abnormalities (including loss of  
696 *IKZF1*) in 40% of cells with disruption of the second copy of *IKZF1* in a further 48% of  
697 cells. No abnormalities were detected in 8% of cells. ^ Indicates both copies of *IKZF1*  
698 are disrupted. All clones were observed in cells isolated from the spleen with the two  
699 most frequent clones being observed in the bone marrow.

700 **(B) Non-DS-ALL patient 21819** - In the diagnostic sample 296 cells were successfully  
701 screened. Bulk diagnostic cells engrafted in three mice and were serially transplanted.  
702 We investigated the spleen and bone marrow from one primary mouse (229 and 237  
703 cells respectfully) and one secondary mouse (76 and 221 cells respectfully). This  
704 leukaemia presented at diagnosis with a linear sub-clonal architecture characterised

705 by multiple aberrations; the deletion of *IKZF1* was sub-clonal (96% of cells). The bulk  
706 sub-clone represented 89% of cells and harboured a *P2RY8-CRLF2* fusion. This sub-  
707 clone was observed across primary and secondary mice (S) in cells harvested from  
708 both the spleen and bone marrow. Primary mice also harboured the smaller sub-  
709 clone.

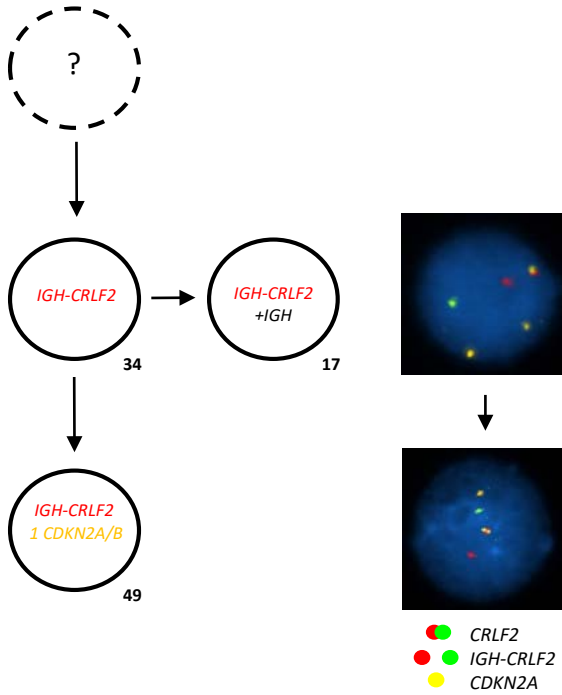
710 **(C) DS-ALL patient 19599** - In the diagnostic sample 257 cells were successfully  
711 screened. Bulk diagnostic cells engrafted in three mice, the spleen and bone marrow  
712 (229 and 237 cells respectively) were investigated from one mouse. At diagnosis three  
713 independent subpopulations evolved from a backbone of clonal aberrations (which  
714 included loss of *IKZF1* and a *IGH-CRLF2* translocation). A small clone observed in 2% of  
715 cells acquired biallelic loss of *IKZF1*. Two further clones acquired unique independent  
716 *IKZF1* mutations each then fostering additional alterations; one losing a single copy of  
717 *BTLA* and gaining a *TOP3A* mutation (13% of cells) followed by the acquisition of a *JAK2*  
718 mutation (54% cells); the other acquired another independent *JAK2* mutation (4% of  
719 cells) followed by a *GNB1* mutation (27%). This was the only clone to be detected in  
720 the mouse spleen and bone marrow cells from the mouse. ^ In those cells with an  
721 *IKZF1* mutation, only the mutant signal was present, confirming *IKZF1* copy number  
722 loss and mutation of the remaining copy.

723 **(D) DS-ALL patient 11538** - In the diagnostic sample 324 cells were successfully  
724 screened. Bulk diagnostic cells engrafted in three mice, the spleen and bone marrow  
725 (243 and 240 cells respectively) were investigated from one mouse. At diagnosis two  
726 independent clones evolved from a very complex backbone of aberrations (including  
727 loss of *IKZF1* and a *P2RY8-CRLF2* fusion). A small clone was characterised by disruption  
728 of the second copy of *IKZF1* alone (7% of cells) compared to the bulk clone which

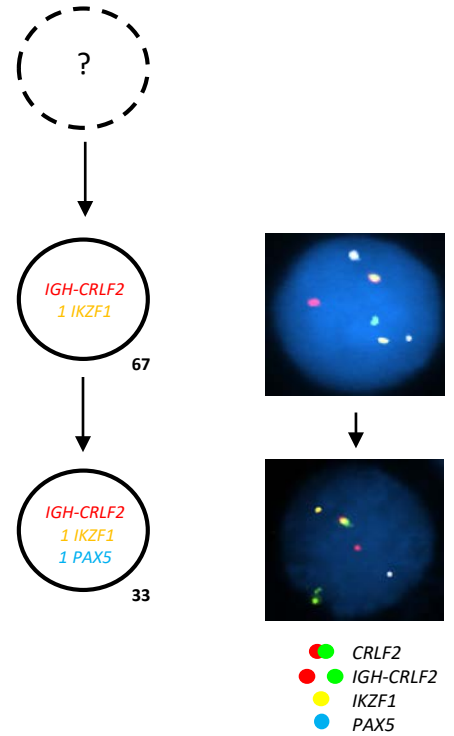
729 acquired 5 further mutations and then disruption of the second copy of *IKZF1* (57% of  
730 cells). ^ Indicates both copies of *IKZF1* are disrupted. All clones were observed in the  
731 cells harvested from mouse spleen and bone marrow. The small clone characterised  
732 by disruption of the second *IKZF1* allele was the major clone appearing in the mice.  
733

**Figure 1. Multiple colour FISH showing examples of *IGH-CRLF2* as a clonal event arising (A) first or (B) together with other tracked abnormalities (C) *P2RY8-CRLF2* as a clonal event arising first or (D) together with other tracked abnormalities.**

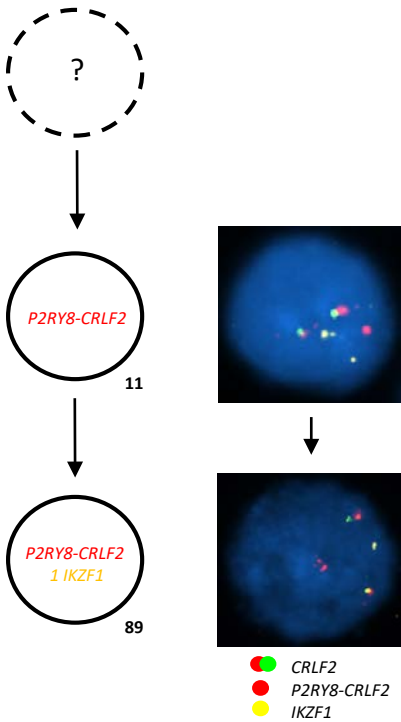
(A) 23394



(B) 4001



(C) 10924



(D) 322

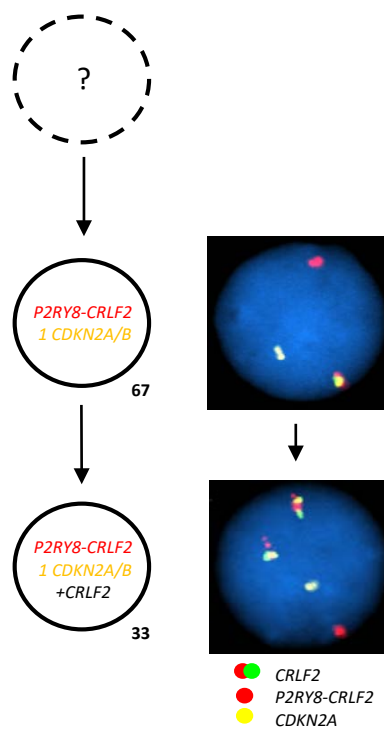
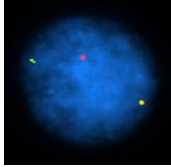
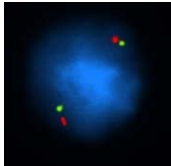


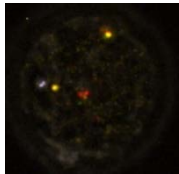
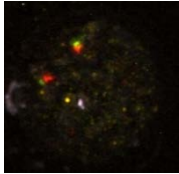
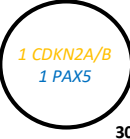
**Figure 2. Multiple colour FISH showing examples of the sub-clonal nature of (A) *P2RY8-CRLF2* (B) *IGH-CRLF2***

(A) 3789



- CRLF2
- IGH-CRLF2
- IKZF1

(B) 2017



- CRLF2
- P2RY8-CRLF2
- CDKN2A/B
- PAX5

**Figure 3. Multiple colour FISH showing examples of parallel evolution in (A-E) *P2RY8-CRLF2* (F) *IGH-CRLF2* patients driven by reiterative CNAs within the same genes**

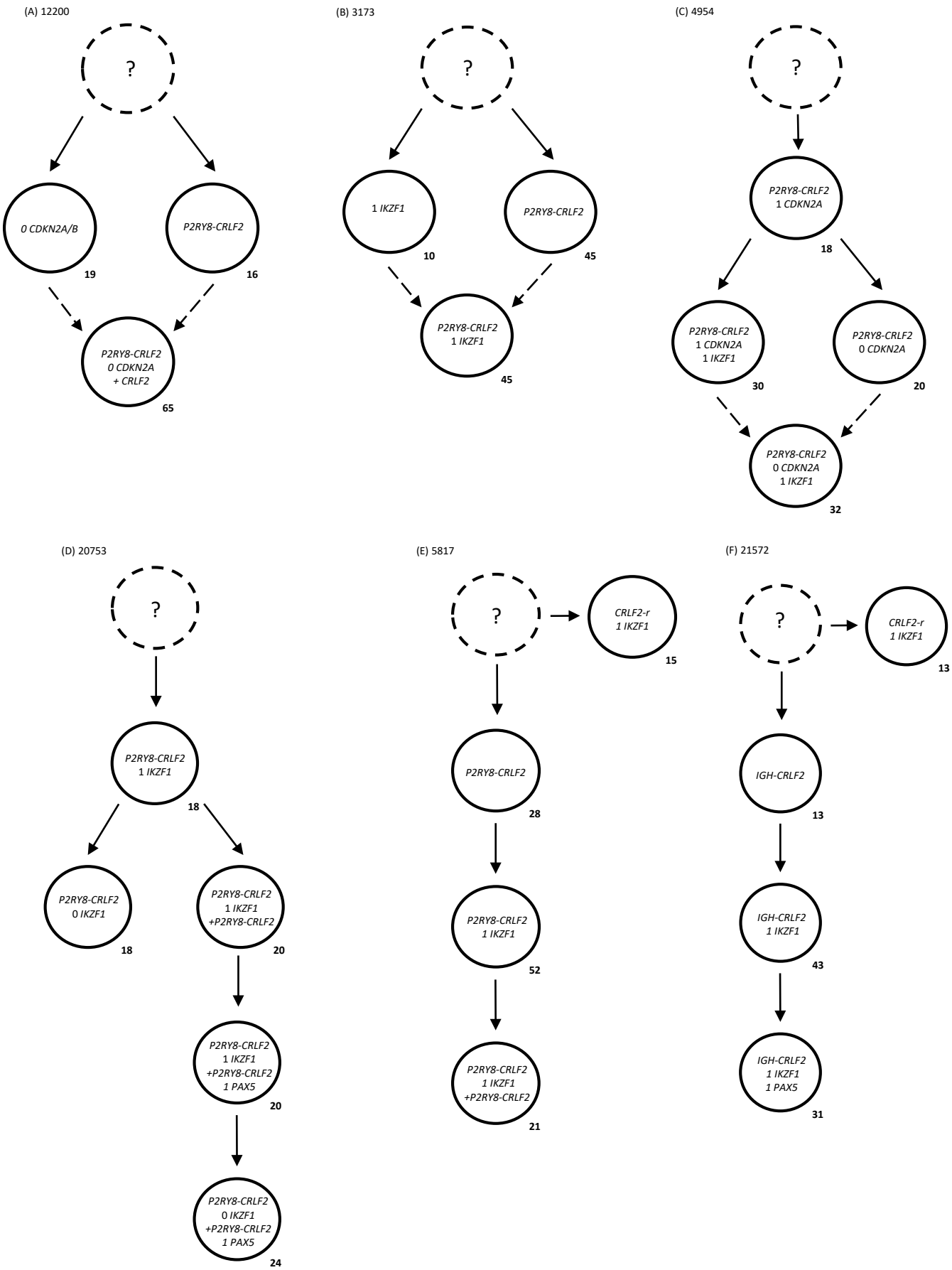




**Figure 4. Sub-clonal architecture demonstrated by single cell analysis**

